Energy Conversion and Management 178 (2018) 322–334

Contents lists available at ScienceDirect

Energy Conversion and Management

journal homepage: www.elsevier.com/locate/enconman

# Techno-economic feasibility of grid-independent residential roof-top solar PV systems in Muscat, Oman

Juman Al-Saqlawi[a,b], Kaveh Madani[a], Niall Mac Dowell[a,b,*]

[a] Centre for Environmental Policy, Imperial College, London, United Kingdom
[b] Centre for Process Systems Engineering, Imperial College, London, United Kingdom

ARTICLE INFO

*Keywords:*
Solar
Photovoltaics
Battery
Energy
Microgeneration

ABSTRACT

Oman is a country characterised by high solar availability, yet very little electricity is produced using solar energy. As the residential sector is the largest consumer of electricity in Oman, we develop a novel approach, using houses in Muscat as a case study, to assess the potential of implementing roof-top solar PV/battery technologies, that operate without recourse to the electricity grid. Such systems target the complete decarbonisation of electricity demand per household and are defined in this study as grid-independent systems. The approach adopted starts with a technical assessment of grid-independent systems that evaluates the characteristics of the solar panel and the battery facility required to provide grid-independence. This is then compared to a similar grid-connected system and any techno-economic targets necessary to enhance the feasibility of residential roof-top PV systems in Muscat are identified. Such an analysis was achieved through developing a detailed techno-economic mathematical model describing four sub-systems; the solar panel DC source, the grid-independent sub-system, the grid-connected sub-system and the economic sub-system. The model was implemented in gPROMS and uses real hourly weather and climate conditions matched with real demand data, over a simulated period of 20 years. The results indicate that, in the context of the system studied, grid-independent PV systems are not feasible. However, combined with a sufficiently high electricity price, grid-independent systems can become economically feasible only with significant reductions in battery costs (> 90% reductions).

## 1. Introduction

The residential sector in Oman is the largest consumer of electricity, where approximately half of the electricity produced in the country goes to the residential sector [1]. Given that the level of solar energy density in Oman is among the highest in the world [2], roof-top PV panels could serve as a solution to reduce reliability on the grid thereby reducing the consumption of natural gas and therefore $CO_2$ emissions. However, one of the major issues with PV systems is that times of peak supply do not necessarily match with times of peak demand. Therefore, energy storage is essential to balance supply and demand [3]. Most studies on PV systems with battery storage, commonly known as off-grid systems, such as those presented by Dufo-Lopez et al. [4], Shezan et al. [5], Yilmaz et al. [6] and Ghafoor and Munir [7], focus on the optimal sizing of these systems in remote areas that are isolated from grid connection and rely on diesel generators for their power supply. Sizing in these studies was based on determining the power and energy rating of the PV and battery facility respectively. Therefore there was no discussion on the physical size of such systems and no analysis on their practicality.

Since extending the national grid to rural areas with existing off-grid systems is a plausible scenario, Bastholm and Fiedler [8] assess the economic viability, but not the practical viability, of maintaining existing off-grid systems. Their results highlight the importance of taking both system loads as well as grid blackouts into consideration. For residential buildings that are already connected to the grid network, and using a similar power and energy rating sizing approach as discussed above, Khoury et al. [9] attempts to optimally size a PV/battery system with the battery as a back-up to the grid instead of diesel generators during power outages. Their key conclusion is that such systems are well-suited to, as well as affordable for, their specific case study of Lebanon. However, since large integration of grid-connected PVs in the network introduces a few technical challenges including the degradation of the voltage profile from the feeder, Ratnam et al. [10] assessed the potential of using battery technologies in residential PV systems to maintain grid voltages within acceptable levels while simultaneously

* Corresponding author at: Centre for Environmental Policy, Imperial College, London, United Kingdom.
*E-mail address:* niall@imperial.ac.uk (N. Mac Dowell).

https://doi.org/10.1016/j.enconman.2018.10.021
Received 20 August 2018; Received in revised form 7 October 2018; Accepted 8 October 2018
Available online 18 October 2018
0196-8904/ 

maximising the daily operational savings that accrue to customers. This was explored for a range of financial incentives offered for PV uptake where it was concluded that the use of battery technologies is advantageous in terms of maintaining grid voltages. However, the feasibility of the proposed PV/battery system was not discussed.

Given that the cost of electrical energy storage systems plays a pivotal role in future low-carbon energy systems, Schmidt et al. [11] constructed experience curves to project future prices for eleven electrical energy storage technologies, including batteries. They found that regardless of technology, although capital costs currently range from 150 to 2000 USD/kWh, they are on a trajectory towards 175 ± 25 USD/kWh for battery packs once 1 TWh of capacity is installed for each technology. Although this price range was confirmed to be feasible by performing a bottom-up assessment of material and production costs, there was no discussion on how these projected costs would impact the feasibility of roof-top PV/systems.

Since complete independence from the grid using roof-top PV/battery systems represents a case whereby the electricity demand per household is completely decarbonised while any excess power produced is stored by a battery instead of being exported to the grid thereby eliminating issues emerging from connecting to the grid such as reverse power flows, this study develops a novel step by step approach on grid-independent systems. This is achieved by developing a model in gPROMS [12] and using Muscat, Oman as a case study, to explore the following gaps that exist in assessing residential roof-top PV systems, mainly PV/battery systems:

- Including physical sizing to the overall sizing analysis of PV/battery systems thereby allowing for the assessment of the practicality of such systems.
- Assessing the impact of varying technical parameters specific to the individual PV and battery technologies on PV/battery system feasibility.
- Setting economic targets necessary to make residential roof-top PV systems economically feasible.
- Evaluating the impact of demand size and demand profile on PV/battery system size.
- Assessing the impact of varying the installation date on PV/battery system size and start-up conditions.
- Understanding how PV/battery system size evolves over time due to factors such as degradation and variations in demand.

This step by step approach starts with a technical analysis of grid-independent systems and ends with an economic analysis where the economic feasibility of a grid-independent system is compared to a similar grid-connected system. The model developed for this study could be divided into four sub-models presented in Section 2 below. These sub-models are applicable to any location and various PV and battery technologies. Section 3 describes the input data used for this specific case study of Muscat. The results obtained are presented in Sections 4 and 5. Finally, these results are analysed in Section 6 where conclusions are drawn.

## 2. Model design and construction

### 2.1. DC source

The core element of a roof-top PV system is the direct current (DC) power output from the PV module ($P_m$), also known as the DC source. Solar radiation is primarily measured as global solar irradiance on a horizontal plane (*GSI*). However, $P_m$ is directly dependent on the solar radiation incident on it ($GSI_T$) [13,14]. $GSI_T$ is determined by geometric parameters such as the tilt angle of the PV from the horizontal surface ($\beta$) and the orientation towards the sun, the latter comprising the declination angle ($\delta$), the elevation angle ($\alpha$) and the latitude ($\phi$) [13]. $\delta$ varies seasonally due to the tilt of the earth on its axis of rotation by 23.45° and the rotation of the earth around the sun. Therefore, $\delta$ is determined by the day of the year ($d$) and can be described by Eq. (1) below [13]:

$$\delta = \sin^{-1}(\sin(23.45°)\sin(\frac{360}{365}(d-81))) \tag{1}$$

The $\alpha$ at solar noon is the maximum $\alpha$ and can be determined by Eq. (2). This maximum $\alpha$ is used in simple PV system design and is used for this model [13].

$$\alpha = \begin{cases} 90-(\phi-\delta), & \text{for locations in the Northern hemisphere} \\ 90+(\phi-\delta), & \text{for locations in the Southern hemisphere} \end{cases} \tag{2}$$

Therefore, given *GSI*, $GSI_T$ can be calculated [13].

$$GSI_T = \frac{GSI\sin(\alpha+\beta)}{\sin(\alpha)} \tag{3}$$

Although Eq. (3) is underestimating $GSI_T$ in terms of not accounting for the increase from the diffuse and reflected irradiance, this is assumed to be acceptable given that this model uses $\alpha$ at its maximum at solar noon, as described by Eq. (2), and therefore is already overestimating $GSI_T$.

Once $GSI_T$ is calculated, the power output of a PV module ($P_m$) can be calculated using:

$$P_m = \eta_m GSI_T \chi A_r [1-n(PVD)] \tag{4}$$

where $A_r$ is the roof area, $\chi$ is the proportion of the roof area covered with PV modules and $\eta_m$ is the efficiency of the module usually approximated as [15]:

$$\eta_m = \eta_{ref}[1-\beta_{ref}(T_c-T_{ref})] \tag{5}$$

where the values of the reference efficiency ($\eta_{ref}$), reference temperature ($T_{ref}$) and the temperature coefficient ($\beta_{ref}$) are normally given by the PV manufacturer. Given that cell temperature ($T_c$) is one of the most important parameters used in assessing the performance of PV systems and their power output, several cell temperature prediction models have been developed. After a review of several models [14,16–22], the nominal operating cell temperature (*NOCT*) model was chosen for this study owing to its simplicity, adequacy of its predicted temperatures for PV applications and wider availability of input data. In the *NOCT* model, the cell temperature is calculated as [14,16–18]:

$$T_c = T_A + \frac{NOCT-20}{800} GSI_T \tag{6}$$

Additionally, since a study by Jordan and Kurtz [23] of approximately 2000 PV panels has shown that PV panels degrade by an annual rate, *PVD* (%), the power output of the PV module is dependent on the age of the system ($n$). Given that a linear degradation model provides a more conservative estimate than an exponential model [24–26], assessing PV panels that degrades linearly was considered more suitable for this study since a conservative estimate of degradation incorporates the worst case scenario.

Finally, the total energy output of the PV module ($E_m$) in kWh is simply the integral of $P_m$ between two periods of time, $t$. This could then be compared to the total energy demand in kWh ($E_D$), calculated as the integral of $P_D$ between two periods of time.

### 2.2. Grid-independent PV system

Fig. 1(a) shows the schematic of the grid-independent PV system model developed for this study [7,27–29]. In this system, the energy produced by the DC source is consumed directly by converting it into AC electricity using an inverter with an efficiency $\eta_{inv}$ and an absolute lifetime $N_{inv}$. Any excess energy is stored in the battery as DC power and any shortfall in energy is provided for by the battery. The battery is protected from overcharge and deep discharge using a charge controller with an efficiency $\eta_{cc}$ [30]. Therefore, within the PV system depicted in

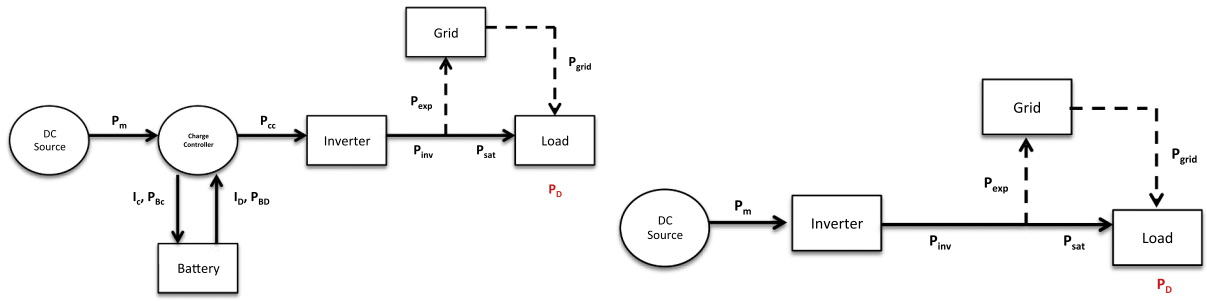


(a) Grid-independent PV system [7, 27]. (b) Grid-connected PV system [13].

**Fig. 1.** Schematic of residential roof-top PV systems.

Fig. 1(a), two situations could exist; a surplus in which the PV system produces more energy than household demand ($P_D$) and a shortfall in which the PV system produces less energy than household demand. Whether the system is in surplus or shortfall is determined by the following equation:

$$P^+ = (\eta_{cc}\eta_{inv})P_m - P_D \tag{7}$$

where $P^+ > 0$ during a surplus and $P^+ < 0$ during a shortfall [31]. If $P^+ = 0$, the battery does not charge or discharge and all power produced is consumed immediately.

### 2.2.1. Surplus ($P^+ > 0$)

Initially, during a surplus, the power generated is used to satisfy demand ($P_{sat}$). This can be expressed by:

$$P_{sat} = P_D \tag{8}$$

The remaining power is then used to charge the battery within its limits. If the battery is not already fully charged, the battery will receive a charge current limited by the maximum charge current, $I_{Cmax}$. The value of the available charge current, $I_{C0}$, at any time (*i.e.* ignoring the state of the battery) is given by:

$$I_{C0} = \frac{P^+}{\eta_{cc}\eta_{inv}V_B} \tag{9}$$

The actual charge current, $I_C$, that accounts for the state of the battery is limited by $I_C \leqslant I_{Cmax}$ as well as $SOC < SOC_{max}$. Therefore, if the battery is full ($SOC = SOC_{max}$) the battery cannot be charged ($I_C = 0$). Otherwise, if $SOC < SOC_{max}$ and $I_{C0} \leqslant I_{Cmax}$, then $I_C = I_{C0}$. If, on the other hand, $SOC < SOC_{max}$ and $I_{C0} > I_{Cmax}$, then $I_C = I_{Cmax}$. Given the battery voltage, $V_B$, the battery charge power, $P_{BC}$, is given by:

$$P_{BC} = I_C V_B \tag{10}$$

The amount of charge gained by the battery during a time period $\Delta t$ or the battery charge capacity, $C_C$, is given by:

$$C_C = (I_C \Delta t)\eta_{batt}^{C} \tag{11}$$

where $\eta_{batt}^{C}$ is the battery charge efficiency. During a surplus, it is possible to export power to the grid if either; $SOC = SOC_{max}$ or $I_{C0} > I_{Cmax}$. The power exported as a result of these conditions, $P_{exp}$ is given by:

$$P_{exp} = P^+ - P_{BC} \tag{12}$$

### 2.2.2. Shortfall ($P^+ < 0$)

In the event of a shortfall, all the power produced is used to satisfy demand. Therefore:

$$P_{sat} = \eta_{inv}(\eta_{cc}P_m + P_{BD}) \tag{13}$$

Furthermore, the battery will meet this shortfall by discharging, up to the specified maximum discharge current, $I_{Dmax}$. The current from the battery that would be required to meet the shortfall in power, $I_{D0}$, is given by:

$$I_{D0} = \frac{-(P_+)}{\eta_{cc}\eta_{inv}V_B} \tag{14}$$

The actual discharge current, $I_D$, accounting for the state of the battery, is limited by $I_D \leqslant I_{Dmax}$ and $SOC > SOC_{min}$. Therefore, if the battery is empty ($SOC = SOC_{min}$), the shortfall is met by the grid. Otherwise, if $SOC > SOC_{min}$, it is prioritised over the grid to meet the shortfall by discharging. In such cases, if $I_{D0} < I_{Dmax}$, then $I_D = I_{D0}$. On the other hand, if $I_{D0} \geqslant I_{Dmax}$, then $I_D = I_{Dmax}$. Given $V_B$, the battery discharge power, $P_{BD}$, is given by:

$$P_{BD} = I_D V_B \tag{15}$$

The amount of charge discharged by the battery during a time period $\Delta t$ or the battery discharge capacity, $C_D$, is given by:

$$C_D = (I_D \Delta t)\eta_{batt}^{D} \tag{16}$$

where $\eta_{batt}^{D}$ is the battery discharge efficiency. Since the grid is presumed available to ensure that the demand is always met when either $SOC = SOC_{min}$ or $I_{D0} > I_{Dmax}$, the power being met by the grid, $P_{grid}$, is given by:

$$P_{grid} = (-P^+) - \eta_{inv}P_{BD} \tag{17}$$

### 2.2.3. Battery state of charge (SOC)

Tracking the battery's state of charge at any given time, $SOC(t)$, can be calculated through tracking the change in battery capacity, $\Delta C$, where:

$$\Delta C = C_C - C_D \tag{18}$$

Negative values of $\Delta C$ result during discharge and positive values during charge. The battery charge, $C(t)$, at any time $t$, is therefore:

$$C(t) = [C(t-1) + \Delta C][1 - BSD_h] \tag{19}$$

where $C(t-1)$ is the charge of the battery during the previous time period and $BSD_h$ is the battery's hourly self-discharge rate. Therefore, the battery's state of charge at any given time, $SOC(t)$, can be calculated using:

$$SOC(t) = \frac{C(t)}{C} \tag{20}$$

This will be limited by the expression $SOC_{min} \leqslant SOC(t) \leqslant SOC_{max}$.

## 2.3. Grid-connected system

The grid-connected system designed is shown in Fig. 1(b) where the PV module is connected to a DC/AC inverter. The inverter efficiency ($\eta_{inv}$) is assumed to be the same as that of the grid-independent system. In a similar manner to the grid-independent system, two situations could exist; a surplus in which the power output from the inverter $P_{inv}$ is greater than $P_D$ and a shortfall in which $P_{inv}$ is less than $P_D$. During a

surplus, some of the power output from the inverter is used to satisfy the demand ($P_{sat} = P_D$) while the surplus power is exported to the grid ($P_{exp} = P_{inv} - P_D$). On the other hand, during a shortfall the power output from the inverter is used to satisfy some of the demand ($P_{sat} = P_{inv}$) while additional power is imported from the grid ($P_{grid} = P_D - P_{inv}$) to satisfy the shortfall. Finally, if $P_{inv} = P_D$, all power produced is consumed immediately.

### 2.4. Economic model

Installing a grid-independent roof-top PV system into a household has the potential to provide a return by eliminating electricity bills. In order to evaluate the attractiveness of this investment to a rational actor, we include an economic analysis in our model using a net present value (*NPV*) analysis as described in Eq. (21) [13,32,33].

$$NPV = \sum_{n=0}^{N} \frac{Cost_{total,n} - Benefit_{total,n}}{(1+r)^n} \tag{21}$$

where $Cost_{total,n}$ and $Benefit_{total,n}$ are the total costs and benefits for year $n$, $r$ is the discount rate and $N$ is the PV system lifetime.

Two parameters used to evaluate the attractiveness of an investment are the pay-back period and the internal rate of return (*IRR*) where the pay-back period measures the length of time required to recover the cost of an investment [13,34,35] while the *IRR* considers the time value of money and determines the interest rate at which the *NPV* equals zero [36].

#### 2.4.1. Costs and benefits

The main costs associated with the grid-independent system are the costs of the individual components of the system as summarised in Table 1, in addition to installation and operation and maintenance costs (O&M). For the grid-connected system, the costs are assumed to be the same as that of the grid-independent system, excluding the cost of the battery and charge controller. In terms of benefits, the main benefit associated with a grid-independent system is an annual reduction in electricity bills. This is calculated using the residential electricity tariff structure. On the other hand, a grid-connected system is considered to have an additional benefit to that of the grid-independent system; due to the export of the surplus energy to the grid.

## 3. Case study input data

The data input into the models described in Section 2 can be divided into two parts; hourly data which is input into the DC source model and parameters that are input into all the models. Both these input data sets are described below.

### 3.1. Hourly input data

Half-hourly demand data for 14 different villas ranging in floor areas between 218 m$^2$ and 858.3 m$^2$, for the year 2013 was collected from [39] for Muscat, Oman. Given the relative paucity of villa data available, a method was devised whereby a model villa with a representative hourly demand covering one year ($P_D$) and an average roof area ($A_r$ = 503 m$^2$) was developed. This was achieved by assessing the demand data collected, taking into consideration demand data coverage and using averaging and extrapolation techniques to establish hourly demand data for one year. In turn, the roof area ($A_r$) was determined using a weighting method that reflects the paucity of the collected data, including variations in villa size and demand data coverage.

**Table 1**
Summary of equations used to calculate the costs and benefits of installing grid-independent and grid-connected systems.

| Cost | Equation | References |
|---|---|---|
| Cost of PV | $Cost_{PV} = UC_{PV} \times MAX(P_m)$ | [7,37,38] |
| Cost of Battery | $Cost_{Battery} = UC_{Batt} \times C \times V_B$ | [3,7] |
| Cost of Inverter | $Cost_{Inverter} = UC_{inv} \times MAX(P_D)$ | [7,28] |
| Cost of Charge Controller | $Cost_{cc} = \frac{MAX(P_m)}{V_B} \times SF \times UC_{cc}$ | [7,28] |
| Installation Cost | $10\% \times Cost_{PV}$ | [7,13] |
| O&M Cost | $2\% \times Cost_{PV}$ | [7,13] |

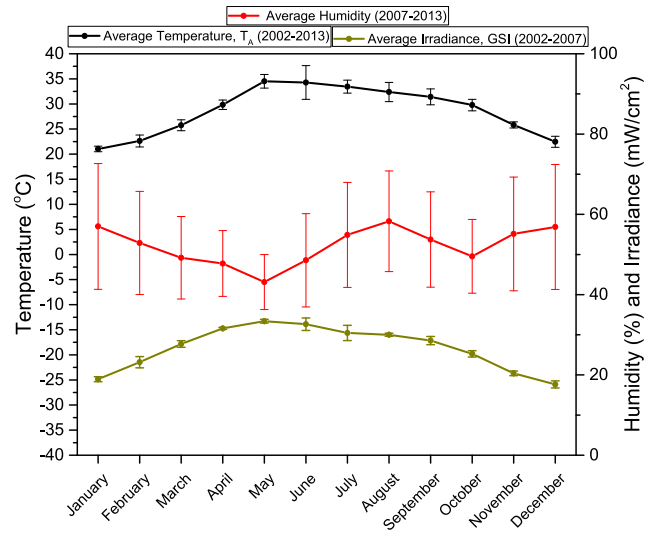


**Fig. 2.** Weather variability in Muscat.

Furthermore, hourly temperature ($T_A$) and *GSI* data for Muscat was collected from [40] where the latest available hourly data was for the year 2007. Since the variation in monthly $T_A$ and *GSI* data for the period covering the years 2002–2013 was found to be small [41,42], as shown in Fig. 2, it was established that it is acceptable to assume that the 2007 hourly weather data was representative of the year 2013.

### 3.2. Input parameters

The specific type of PV technology that was studied is the crystalline-silicon (c-Si) module as this is a mature technology which dominates the market with an 85–90% share [13]. The tilt angle ($\beta$) needed to be input into Eq. (3) was determined by assuming that $\beta$ is changed manually on a monthly basis to achieve maximum monthly power output ($P_m$). These tilt angles are summarised in Fig. 3. Furthermore, the lead-acid battery was chosen as the energy storage technology due to its maturity and low cost [43]. The charge/discharge efficiency, $\eta^C_{batt}/\eta^D_{batt}$, of this battery were modelled according to a relationship described by Jenkins et al. [31] for lead-acid batteries as shown in Eq. (22) below.

$$\eta^{C,D}_{batt} = \frac{100}{13.3 ln \frac{CV_B}{I_{C,D}} + 59.8} \tag{22}$$

The profits from the export of electricity to the grid was calculated using Oman's residential electricity tariff structure [44]. Tables B.2–B.4 summarise the list of key parameters input into the DC source model, the grid-independent and grid-connected models and the economic model respectively.

## 4. Results

### 4.1. Technical results

#### 4.1.1. Supply vs demand

Before determining whether an individual dwelling in Muscat can become grid-independent, it is necessary to understand whether power

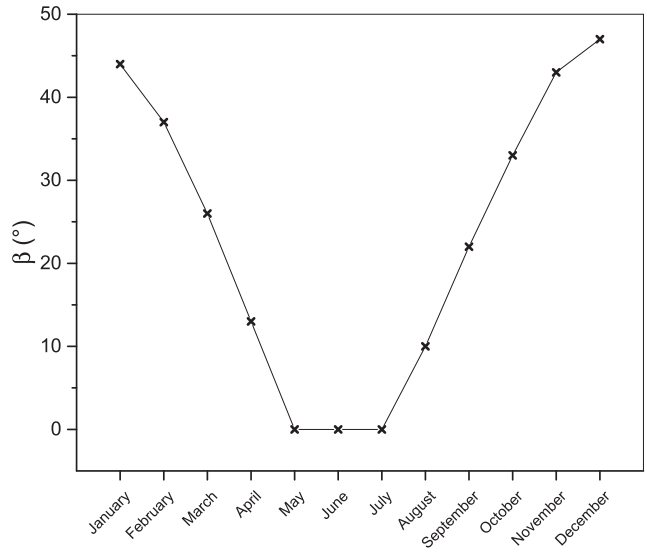


**Fig. 3.** Optimum tilt angle ($\beta$) per month in Muscat.

supply from roof-top PV panels can ever exceed the current demand. Fig. 4(a) shows how the annual $E_m/m^2$ from roof-top PV increases as the roof area coverage, $\chi$, increases. The error bars show how $E_m/m^2$ would vary as *PVD* changes between 0% and 2.5% [23]. This chart clearly shows that at the median *PVD* of 0.7%, supply can exceed demand when 33% of the roof is covered. However, this value can go as high as 55% when *PVD* = 2.5%. Once the $\chi$ needed for supply to exceed demand was determined, the monthly variations of $E_m/m^2$ and $E_D/m^2$ at $\chi$ = 33% and *PVD* = 0.7% were determined and are presented in Fig. 4(b). Additionally, the error bars show how the value of $E_m/m^2$ at $\chi$ = 33% would vary as *PVD* changes between 0% and 2.5%. This chart shows that for seven months of the year, supply exceeds demand. However, in the summer months, particularly July and August, the demand increases by a factor of six since both humidity and temperature are high during these months, as shown in Fig. 2, leading to increased demand for cooling [45].

#### 4.1.2. One year of grid independence: changing PVD and BSD

Following the assessment of $E_m/m^2$ versus $E_D/m^2$, the potential of an individual dwelling in Muscat to become grid-independent was examined. It must be noted that in this study, grid-independent status was defined as the point at which no power is imported from or exported to the grid ($P_{grid} = P_{exp} = 0$). This was initially achieved by determining the characteristics needed for a system; which starts running with an empty battery on the 1st of January mid-day and runs for one year, to become grid-independent. The specific year chosen in this assessment was the final year of the project (*i.e.*, at $n = N - 1$) since the system is at its most degraded state in the final year. This choice is necessary since the roof area coverage needed to become grid-independent in the final year is the minimum needed by the system to cover demand throughout its lifetime. Therefore the characteristics determined in this assessment include the roof area coverage ($\chi_{GI}$) and the battery size ($C^{GI}$) needed to be grid-independent for one year. The impact of changing the *PVD* and *BSD* on $\chi_{GI}$ and $C^{GI}$ is shown in Fig. 5.

From Fig. 5(a), it can be seen that the minimum $\chi$ needed to achieve grid-independent status is larger than the 33% determined in Section 4.1.1. This is mainly due to the fact that Section 4.1.1 does not take into consideration losses due to the inverter, charge controller and battery. Therefore, at the current *PVD* of 0.7% and *BSD* of 5%, grid-independent status at year $n = N - 1$ can be achieved with $\chi_{GI}$ = 40% and $C^{GI}$ = 165 kAh. It can further be observed that while both *PVD* and *BSD* have an impact on minimising $\chi_{GI}$, reducing *BSD* results in a bigger $C^{GI}$ requirement. The impact of *PVD* and *BSD* on $\chi_{GI}$ is due to the fact that these variables impact the amount of power available for use. Thus, the higher *PVD* and/or *BSD*, the larger the power losses which means additional power is needed to be produced, therefore $\chi_{GI}$ is higher. On the other hand, reducing *BSD* increases the amount of charge the battery needs to store resulting in a greater battery size requirement. Since a reduction of *PVD* results in a reduction in $\chi_{GI}$ but maintains the amount of energy produced, its impact on $C^{GI}$ is minimal. These results indicate that in order to reduce the grid-independent system size in Muscat, *PVD* needs to be reduced but a balance in *BSD* needs to be found whereby both $\chi_{GI}$ and $C^{GI}$ are minimised.

#### 4.1.3. One year of grid independence: changing solar PV efficiency ($\eta_{ref}$)

The analysis of the previous section assessed the impact of changing *PVD* and *BSD* on $\chi_{GI}$ and $C^{GI}$. This section assesses the impact of changing the solar PV efficiency ($\eta_{ref}$) with results illustrated in Fig. 6 where increasing $\eta_{ref}$ from its current 12% to the Shockley-Queisser limit of 33% [46] reduces the roof area coverage by about 60%. Although more efficient solar panels tend to be more expensive [47], PV prices are impacted by various other factors such as economies of scale and automation. Therefore, if the prices are assumed to remain the same, this in turn would mean a 60% reduction in PV capital costs.

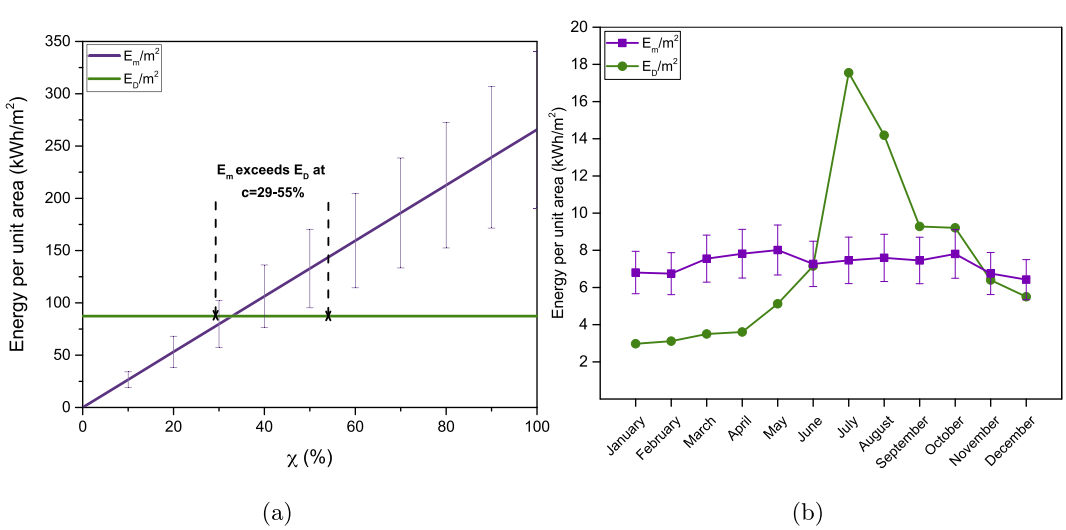


**Fig. 4.** Graphs showing if solar PV supply in Muscat can exceed demand at the median *PVD* of 0.7% where (a) shows the change in annual $E_m/m^2$ and $E_D/m^2$ with $\chi$ while (b) shows the monthly $E_m/m^2$ and $E_D/m^2$ at $\chi$ = 33%. The error bars show how $E_m/m^2$ would vary as *PVD* changes between 0% and 2.5% [23].

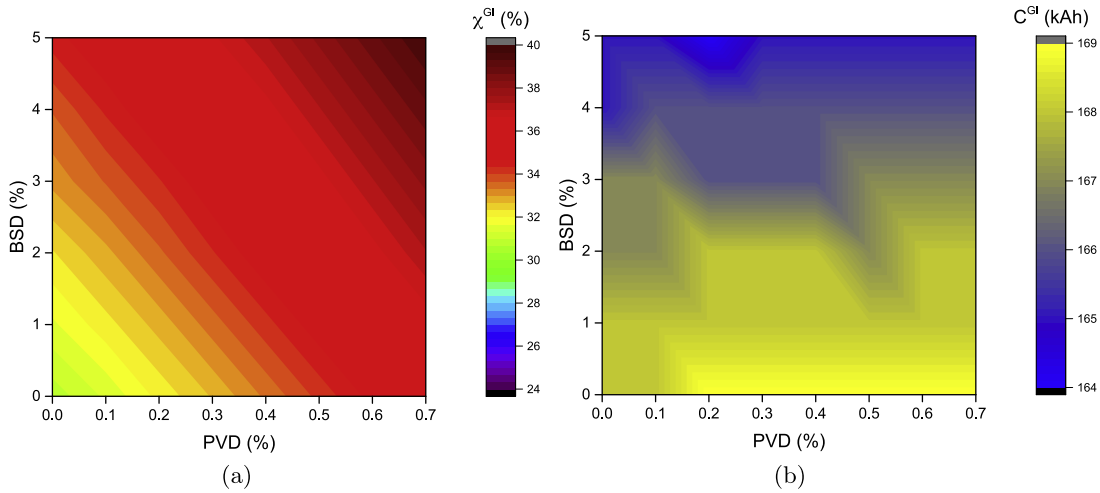


**Fig. 5.** Graphs showing the impact of changing *PVD* and *BSD* on the grid-independent system characteristics in Muscat for year $n = N - 1$ where (a) shows how $\chi_{GI}$ is impacted and (b) shows how $C^{GI}$ is impacted.

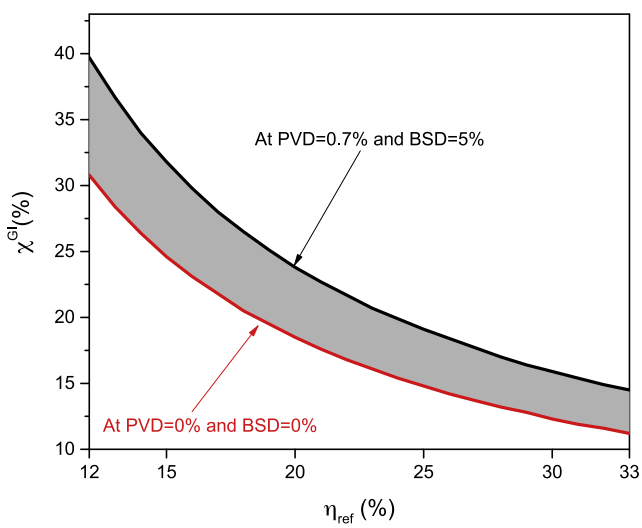


**Fig. 6.** Graph showing the impact of changing the solar PV efficiency ($\eta_{ref}$) of a grid-independent system in Muscat from its current 12% to the Shockley-Queisser limit of 33% on $\chi_{GI}$ [46].

#### 4.1.4. One year of grid independence: differing installation dates

PV/battery systems are expected to be installed anytime therefore in order to assess the impact of battery installation dates on grid-independent system characteristics as compared to January, three different points of year $n = N - 1$ (March, July and September) were chosen. As can be seen from Fig. 7, the time you install and start running the grid-independent system in Muscat matters. Installing the system in January requires an empty battery of size $C^{GI} = 165$ kAh while installing the system in July requires a larger battery ($C^{GI} = 191$ kAh) that is pre-charged ($SOC_{initial} = 98\%$). This is due to the fact that in January supply exceeds demand and therefore the battery is in 'charging' mode whereas in July demand exceeds supply and therefore the battery is in 'discharging' mode. Therefore the system installation characteristics is largely driven by the demand profile and thus the less varied the demand is throughout the year, the less varied will be the system characteristics needed to achieve grid-independent status.

#### 4.1.5. Five years of grid independence

All previous analyses considered how to achieve grid-independent status by running the system for one year. However, given that the battery is assumed to have a lifetime of five years (Table C.5), it is important to determine the point at which the system achieves grid-independent status whilst running continuously for five years. Since the previous assessment considered the final year of the project, the five years chosen in this assessment are the final five years of the project (*i.e.*, from $n = N - 5$ to $n = N - 1$). By simulating a system that starts running on the first day of January, mid-day for five years, it is clear that there is an annual variation in $SOC_{initial}$ as shown in Fig. 8, where in the first year $SOC_{initial}$ builds up reducing the available storage space and in the consecutive years, $SOC_{initial}$ reduces due to an increased annual discharge range. This reduction in $SOC_{initial}$ is due to *PVD*, since

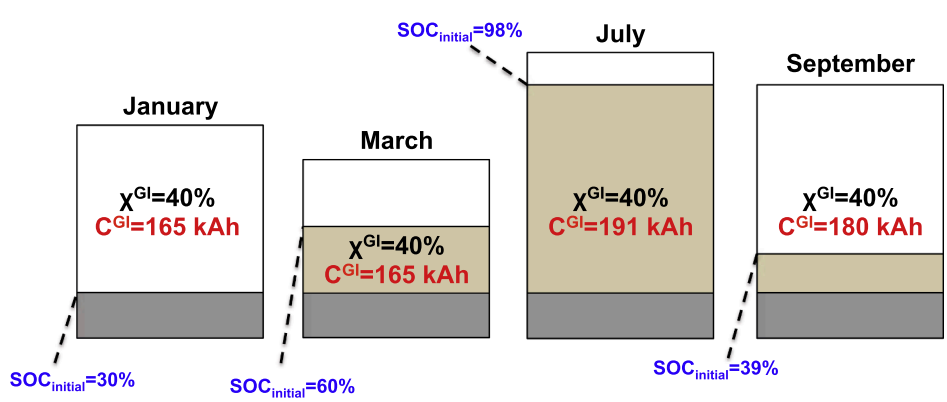


**Fig. 7.** Image depicting the battery specifications needed to achieve grid-independent status in Muscat at four different installation dates of year $n = N - 1$; January, March, July and September.

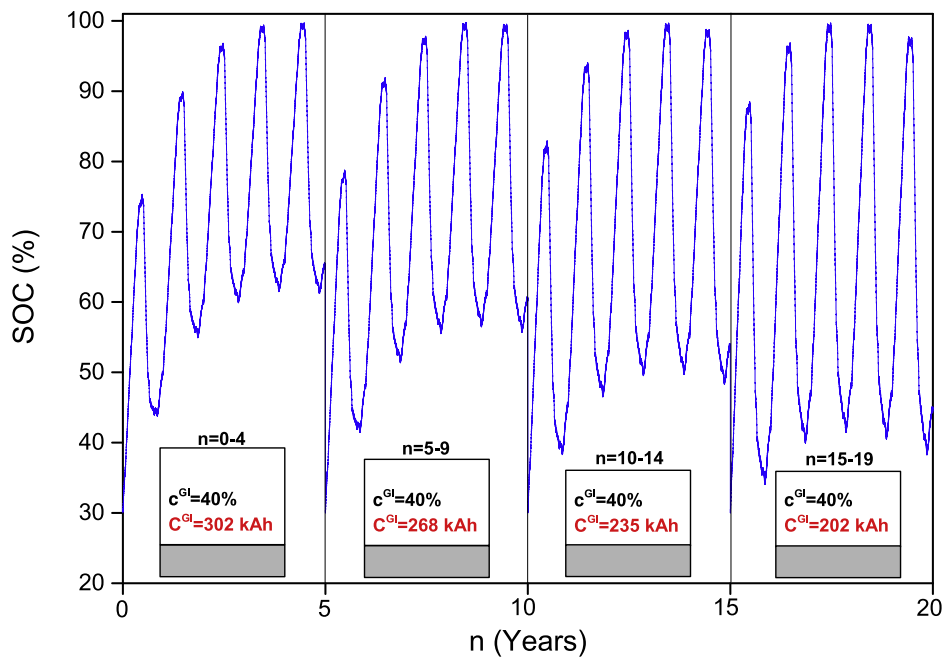


**Fig. 8.** Graph showing the minimum $C^{GI}$ needed for the system in Muscat to be grid-independent at four different points within its 20 year lifetime (*i.e.*, at $n = 0$, $n = 5$, $n = 10$ and $n = 15$). The change in *SOC* of the batteries throughout the 20 years is also shown by the blue line.

every year, the PV panel produces less power causing the battery to discharge slightly more power in order to satisfy the demand. When $PVD = 0\%$, this decline in $SOC_{initial}$ does not exist. Since increased charge/discharge ranges put a strain on battery lifetime [29], it can be concluded that increased *PVD* impacts the lifetime of the battery. Additionally, given the fact that the PV panels are less degraded in the previous years implies that for $\chi_{GI} = 40\%$, excess energy is produced. This combination of factors indicate that a 165 kAh battery is not big enough to achieve grid-independent status and therefore a bigger battery is needed ($C^{GI} = 202$ kAh) in order to be as independent from the grid as possible.

#### 4.1.6. Twenty years of grid independence

The analysis in Section 4.1.5 looked at sizing the grid-independent system for the final five years of the system lifetime. Given that the grid-independent system is assumed to have a lifetime, *N*, of 20 years (Table C.5), the batteries should be expected to be replaced four times (*i.e.*, at $n = 0$, $n = 5$, $n = 10$ and $n = 15$). Assuming $\chi_{GI}$ remains at 40% throughout the system lifetime, $P_m$ will reduce annually due to *PVD*. Therefore the battery size, $C^{GI}$, for the first five years will be higher than that for the final five years due to the excess power produced. This is shown in Fig. 8 which shows the minimum battery sizes needed for the system to be grid-independent at four different points within its lifetime. This chart also shows how the state of charge (*SOC*) of the batteries changes in 20 years depicting clearly how the battery discharge range increases annually due to *PVD*.

## 5. Economic results

### 5.1. Grid-connected system vs grid-independent system-increasing electricity prices

Fig. 9 compares the *NPV* of a grid-connected system in Muscat with that of a grid-independent system and shows the impact of increasing the price of electricity on the economic feasibility of both grid-connected and grid-independent systems. It must be noted that these results are for a system which is assumed to start running in January, mid-day. The battery sizes for the grid-independent system at $PVD = 0.7\%$ and $BSD = 5\%$ are those summarised in Fig. 8. Furthermore, given that the cost of batteries is expected to decrease exponentially over the years at an annual rate ranging between 8 and 14% [48,49], the cost of the batteries was assumed to reduce annually by 11%.

As can be seen from Fig. 9, it is clear that both grid-connected and grid-independent systems in Muscat are not feasible since the *NPV* remains negative throughout the system lifetime. This can be explained by comparing Oman's residential electricity price with the rest of the world. Owing primarily to extensive government subsidy [50], at 2.5 U.S. cents per kWh, the electricity price in Oman is very low, where it is 15 times lower than that of Germany and 5 times lower than the United States [51]. This low electricity price indicates that the benefits that come from PV investments are insufficient to out-weigh the costs therefore making the investment infeasible. Secondly, grid-independent systems are approximately 40 times less feasible than grid-connected systems. This is largely driven by the high battery costs, which form over 97% of the total system cost. Therefore, increasing the price of electricity to 5.94 times the current tariff, at an average price similar to that of United States [51] and Oman's cost-reflective tariff [1], makes grid-connected systems feasible with a pay-back period of ten years. On the other hand, given that grid-independent systems have significantly larger up-front costs, the increase in electricity price needed to break-even is much higher than that for grid-connected systems, with a required increase of 338.70 times the current tariff in order to achieve a pay-back period of ten years. This tariff is over 21 times higher than most countries in the world indicating that an increase in electricity price alone is not enough to make grid-independent systems feasible in Muscat [50].

### 5.2. Grid-connected system vs grid-independent system-technology cost reduction

Fig. 10 shows the combined impact of increasing electricity prices and reducing the unit cost of the PV panel ($UC_{PV}$) on the internal rate of return (*IRR*) of grid-connected systems (Fig. 10(a)) and grid-independent system (Fig. 10(b)) in Muscat. The international electricity prices corresponding to the price increase factors are marked [50]. Additionally, the *IRR* needed for these investments to become feasible for a private investor at $IRR = 13\%$ (red-line), a pension fund at $IRR = 8\%$ (black-line) and the government at $IRR = 4\%$ (blue-line) are

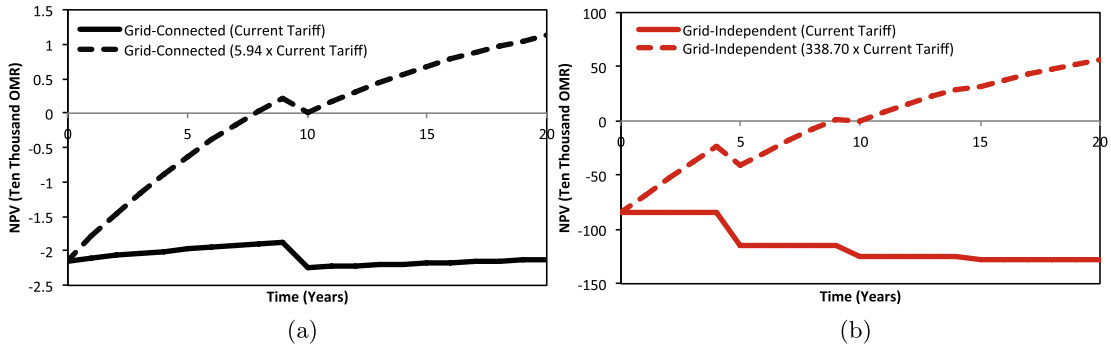


**Fig. 9.** Graphs showing the impact of increasing electricity prices in Muscat on the *NPV* where the dashed lines show the price increases needed to achieve a pay-back period of ten years for (a) grid-connected systems and (b) grid-independent systems.

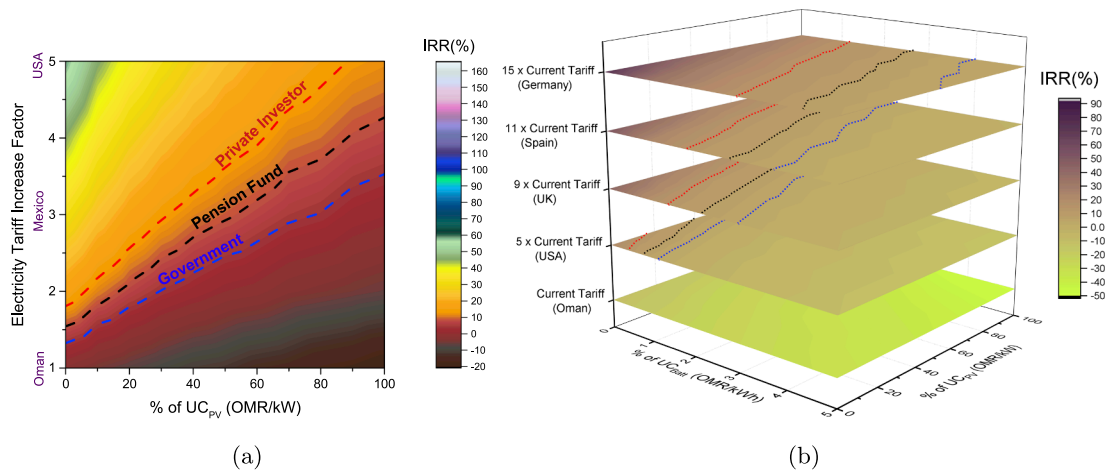


**Fig. 10.** Charts showing the combined impact of increasing electricity prices, reducing the unit cost of the PV panel ($UC_{PV}$) and reducing the unit cost of the battery ($UC_{Batt}$) on the internal rate of return (*IRR*) of (a) grid-connected systems and (b) grid-independent systems in Muscat. The *IRR* needed for these investments to become feasible for a private investor at *IRR* = 13% (red-line), a pension fund at *IRR* = 8% (black-line) and the government at *IRR* = 4% (blue-line) are marked.

marked. These *IRR* values were based on previous work [36].

From Fig. 10(a), it is clear that in addition to the phasing out of subsidies and therefore increasing electricity prices, reducing the cost of the PV plays a significant role in increasing the feasibility of grid-connected systems in Muscat. Although at the current tariff large reductions in $UC_{PV}$ are needed to make grid-connected systems feasible, combined with increasing electricity prices, the reduction in $UC_{PV}$ doesn't necessarily need to be large; where a 20% reduction makes grid-connected systems attractive to private investors when the electricity price in Muscat is lower than the USA average. Given that PV costs are forecast to drop by 10–23% per year within the next fifteen years due to factors such as the reduction in the price of poly-silicon, improvements in technology and increases in industry investment [52,53], these results indicate that these factors should be sufficient to drive PV costs to levels that enhance the feasibility of grid-connected systems in Muscat.

On the other hand, Fig. 10(b) shows that although a reduction in PV cost increases the feasibility of grid-independent systems, it is the reduction in battery cost that has a more significant impact on the feasibility of grid-independent systems since battery cost constitutes 97% of the total cost of grid-independent systems in Muscat. Additionally, it is clear from this chart that at the current electricity price, grid-independent systems are infeasible in Muscat at any $UC_{Batt}$ and $UC_{PV}$ where the *IRR*s are always negative. However, combined with an increase in electricity price, grid-independent systems can become economically feasible with significant reductions in $UC_{Batt}$; where increasing prices to Germany's average requires the battery price to drop by 93–94% (*i.e.* 6–7% of $UC_{Batt}$) which is equivalent to 10–11 USD/kWh. When compared to the forecast in battery price reductions as explored by Schmidt et al. [11], where battery packs are forecast to drop to 175 ± 25 USD/kWh once 1 TWh of capacity is installed, it is clear that increased production and economies of scale are not enough to achieve such price reductions and that further research in technology innovation is necessary.

## 6. Discussion and conclusions

When compared to other countries in the world, such as the USA at 12 MWh/hh.yr, Australia at 7 MWh/hh.yr and the UK, Germany and Spain all at approximately 4 MWh/hh.yr [54], it is evident that Oman's annual electricity consumption per household at 44 MWh/hh.yr is amongst the highest in the world. In turn, this study has shown that household demand in Oman is mainly driven by cooling demand, where the demand profile follows a similar trend to the temperature and humidity profiles. This similarity in profiles indicates that there is a behavioural aspect to the high household demand in Oman, which in turn could be driven by the country's low electricity prices. Therefore, in addition to focusing on the architecture of households, insulation and efficiency measures as well as cooling technologies used, further thought needs to be put into the phasing out of electricity subsidies in Oman as well as altering the electricity tariff structure in order to influence behaviour and reduce demand [55].

Secondly, the combination of high household demand, low electricity prices and high battery cost renders grid-independent systems infeasible in Muscat. The high demand results in a larger overall system size and therefore larger upfront costs, 97% of which is the cost of the battery. Even increasing the PV panel efficiency to its maximum

theoretical efficiency does little to bring down this capital cost. In turn, reducing the unit cost of the battery can make grid-independent systems feasible in Muscat provided electricity tariffs are increased to that of Germany's average. However, this reduction needs to be significant (93–94%) indicating that an increased installation capacity alone is not sufficient to achieve such price reductions and that further research in technology innovation is necessary.

Furthermore, a larger system size not only makes grid-independent systems economically infeasible, but also makes them practically infeasible. It was found that in order to have a 302 kAh system for five years, assuming that each battery has a capacity of 2.4 kWh and weight of 75 kg/kWh [56], 6040 batteries are needed that have a total weight of 1087 tonnes occupying about 13% of the house [57–60]. Not only would storing such a large and heavy amount of batteries prove difficult but the need to maintain them at ambient temperature could result in further increasing the electricity demand. Similarly, changing the battery type to one with a higher energy capacity such as a lithium-ion battery (8–10 kWh) implies that although a reduced amount of batteries are needed, *i.e.* approximately 1610 batteries weighing about 181 tonnes (12.5 kg/kWh), these numbers are still quite high. Additionally, lithium-ion batteries tend to be 2.5–3 times more expensive than lead-acid batteries [56]. Furthermore, lithium itself is a non-renewable, finite product which makes this option less attractive in the long term. On the other hand, low electricity prices imply that the benefits from grid-independent systems cannot outweigh the costs. The fact that a large increase in electricity prices is needed to make grid-independent PV systems economically feasible implies that in order to make such investments feasible, in addition to an increase in electricity tariffs, other PV support policies such as grants and loans are needed [61–63].

Finally, the fact that an increase in electricity price to an average price lower than other PV successful countries such as Germany and Spain makes grid-connected PV systems economically feasible with a pay-back period of less than ten years despite there being no PV support policies such as feed-in-tariffs (FITs) and the household demand in Oman being very high demonstrates the potential of residential grid-connected systems in Oman [61–63]. Furthermore, small reductions in PV cost as a result of increased installation capacity and industry improvements would only make grid-connected systems more feasible in Oman. However, the successful implementation of such systems requires well thought out policies as part of a national energy and renewable energy strategy, with well thought out action plans and designated institutions which assist in permit attainment, finance, behavioural awareness, and research. To date, such policies still do not exist in Oman [61–64].

## Acknowledgments

We thank the Ministry of Higher Education-Oman (MOHE) for the funding of this project.

## Appendix A. Nomenclature

*Acronyms*

| | |
|---|---|
| *AC* | Alternating current |
| *c−Si* | Crystalline-silicon |
| *DC* | Direct current |
| *FIT* | Feed-in-Tariff |
| *OMR* | Omani rial |
| *PV* | Photovoltaic |

*Greek symbols*

| | |
|---|---|
| $\alpha$ | Elevation angle (°) |
| $\beta$ | Tilt angle of the PV from the horizontal surface (°) |
| $\beta_{ref}$ | Temperature coefficient ($K^{-1}$) |
| $\chi$ | Proportion of roof area covered by PV modules (%) |
| $\delta$ | Declination angle (°) |
| $\Delta C$ | Change in battery capacity (kAh) |
| $\Delta t$ | Time period (hours) |
| $\eta_{coulomb}$ | Battery coulombic efficiency (%) |
| $\eta_{voltage}$ | Battery voltage efficiency (%) |
| $\eta_{batt}^{C}$ | Battery charge efficiency (%) |
| $\eta_{batt}^{D}$ | Battery discharge efficiency (%) |
| $\eta_{batt}$ | Battery energy efficiency (%) |
| $\eta_{cc}$ | Efficiency of charge controller (%) |
| $\eta_{inv}$ | Efficiency of inverter (%) |
| $\eta_{m}$ | Efficiency of PV module (%) |
| $\eta_{ref}$ | PV module's electrical efficiency at $T_{ref}$ and solar radiation of 1000 W/m$^2$ (%) |
| $\phi$ | Latitude (°) |

*Roman symbols*

| | |
|---|---|
| $GSI_T$ | Global solar irradiance on a tilted surface (kW/m$^2$) |

| | |
|---|---|
| $GSI$ | Global solar irradiance on a horizontal plane (kW/m$^2$) |
| $P_m$ | Power output of PV module (kW) |
| $A_m$ | Area of PV module (m$^2$) |
| $A_r$ | Roof area (m$^2$) |
| $Benefit_{total,n}$ | Sum of all benefits for year n (OMR) |
| $C$ | Maximum capacity of battery or battery size (kAh) |
| $C(t)$ | Battery charge at time t (kAh) |
| $C(t-1)$ | Battery charge at time t − 1 (kAh) |
| $C_C$ | Charge input into battery during charge (kAh) |
| $C_D$ | Charge removed from battery during discharge (kAh) |
| $Cost_{Battery}$ | Cost of battery (OMR) |
| $Cost_{cc}$ | Cost of charge controller (OMR) |
| $Cost_{Inverter}$ | Cost of inverter (OMR) |
| $Cost_{PV}$ | Cost of PV module (OMR) |
| $Cost_{total,n}$ | Sum of all costs for year n (OMR) |
| $d$ | Day of year |
| $E_D$ | Energy demand (kWh) |
| $E_m$ | Energy output of PV module (kWh) |
| $I_{C0}$ | Available charge current (kA) |
| $I_{Cmax}$ | Maximum allowed charge current (kA) |
| $I_C$ | Actual charge current (kA) |
| $I_{D0}$ | Available discharge current (kA) |
| $I_{Dmax}$ | Maximum allowed discharge current (kA) |
| $I_{DT}$ | Diffuse irradiance on a tilted surface (kW/m$^2$) |
| $I_D$ | Actual discharge current (kA) |
| $I_{RT}$ | Reflected irradiance on a tilted surface (kW/m$^2$) |
| $MAX$ | Maximum |
| $N$ | PV system lifetime (years) |
| $n$ | Age of PV system (years) |
| $N_{Batt}$ | Battery absolute lifetime (years) |
| $N_{inv}$ | Inverter absolute lifetime (years) |
| $NOCT$ | Nominal operating cell temperature (°C) |
| $NPV$ | Net present value (OMR) |

| | |
|---|---|
| $P_{BC}$ | Battery charge power (kW) |
| $P_{BD}$ | Battery discharge power (kW) |
| $P_D$ | Power demand of residential building (kW) |
| $P_{exp}$ | Power exported to the grid (kW) |
| $P_{grid}$ | Power imported from the grid (kW) |
| $P_{inv}$ | Power output from the inverter (kW) |
| $P_{sat}$ | PV generated power and battery power used to satisfy demand (kW) |
| $P^+$ | Surplus power in grid-independent system (kW) |
| $PVD$ | PV annual degradation rate (%) |
| $r$ | Discount rate (%) |
| $SF$ | Charge controller safety factor |
| $SOC$ | Battery's state of charge (%) |
| $SOC(t)$ | Battery state of charge at time t (%) |
| $SOC_{initial}$ | Battery's initial state of charge (%) |
| $SOC_{max}$ | Battery's maximum allowed state of charge (%) |
| $SOC_{min}$ | Battery's minimum allowed state of charge (%) |
| $t$ | Time (hours) |
| $T_A$ | Ambient temperature (°C) |
| $T_c$ | Temperature of PV cell (°C) |
| $T_{ref}$ | Reference temperature (°C) |
| $UC_{Batt}$ | Unit cost of battery (OMR/kWh) |
| $UC_{cc}$ | Unit cost of charge controller (OMR/kA) |
| $UC_{inv}$ | Unit cost of inverter (OMR/kW) |
| $UC_{PV}$ | Unit cost of PV module (OMR/kW) |
| BSD | Battery self-discharge rate per month (%) |
| $BSD_h$ | Battery self-discharge rate per hour (%) |
| $V_B$ | Battery voltage (V) |

## Appendix B. List of key input parameters

See Tables B.2–B.4.

**Table B.2**
List of key inputs required for DC source model.

| Key Model Inputs | Value | Unit | Nomenclature | References |
|---|---|---|---|---|
| Global Solar Irradiance | – | kW/m$^2$ per hour | $GSI$ | [40] |
| Ambient Temperature | – | °C per hour | $T_A$ | [40] |
| Day of Year | – | per hour | $d$ | [40] |
| Latitude | 23.6 | Degrees (°) | $\phi$ | [40] |
| Tilt Angle | – | Degrees (°) | $\beta$ | [40] |
| Electrical Efficiency of PV module | 12 | % | $\eta_{ref}$ | [15] |
| Temperature Coefficient | 0.004 | K$^{-1}$ | $\beta_{ref}$ | [15] |
| Reference Temperature | 25 | °C | $T_{ref}$ | [15] |
| Nominal Operating Cell Temperature | 48 | Degrees (°) | $NOCT$ | [18] |
| Power Demand of Residential Building | – | kW per hour | $P_D$ | [1,39,58] |
| PV Degradation Rate | 0.7 | % per year | $PVD$ | [31] |
| Roof Area | 503 | m$^2$ | $A_r$ | [57,58,65] |
| Proportion of Roof Area Covered with PV Module | – | % | $\chi$ | [13] |

**Table B.3**
List of key inputs required for grid-independent and grid-connected PV system models.

| Key model inputs | Value | Unit | Nomenclature | References |
|---|---|---|---|---|
| Charge Controller Efficiency | 98 | % | $\eta_{cc}$ | [28,30,31] |
| Inverter Efficiency | 94 | % | $\eta_{inv}$ | [14] |
| Inverter Absolute Lifetime | 10 | years | $N_{inv}$ | [7,28] |
| Battery Voltage | 48 | V | $V_B$ | [28–30,43] |
| Maximum Allowed Charge Current | C/10 | kA | $I_{Cmax}$ | [29] |
| Maximum Allowed Discharge Current | C/10 | kA | $I_{Dmax}$ | [29] |
| Maximum Allowed State of Charge | 100 | % | $SOC_{max}$ | [29,31] |
| Minimum Allowed State of Charge | 30 | % | $SOC_{min}$ | [29–31] |
| Initial State of Charge | – | % | $SOC_{initial}$ | [23] |
| Battery Self-Discharge Rate | 5 | % per month | $BSD$ | [66] |
| Battery Hourly Self-Discharge Rate | – | % per hour | $BSD_h$ | [66] |
| Battery Charge/Discharge Efficiency | – | % | $\eta^C_{batt}/\eta^D_{batt}$ | [59,60] |
| Battery Absolute Lifetime | 5 | years | $N_{Batt}$ | [31,67] |

**Table B.4**
List of key inputs required for economic model.

| Key model inputs | Value | Unit | Nomenclature | References |
|---|---|---|---|---|
| PV System Lifetime | 20 | Years | $N$ | [7,13,31] |
| Discount Rate | 7.55 | % | $r$ | [2] |
| Maximum PV Power Output | – | kW | MAX($P_m$) | – |
| Maximum Demand | – | kW | MAX($P_D$) | [39,58] |
| Unit Cost of PV | 400 | OMR/kW | $UC_{PV}$ | [68–73] |
| Unit Cost of Battery | 57 | OMR/kWh | $UC_{Batt}$ | [68–73] |
| Unit Cost of Charge Controller | 1350 | OMR/kA | $UC_{cc}$ | [68–73] |
| Unit Cost of Inverter | 260 | OMR/kW | $UC_{inv}$ | [68–73] |
| Safety Factor | 1.25 | – | $SF$ | [7,28] |

## Appendix C. List of model/input data assumptions and reasoning

See Table C.5.

**Table C.5**
List of model/input data assumptions and reasoning.

| Assumptions | Reasoning |
|---|---|
| $I_{DT}$ and $I_{RT}$ are negligible | Most monitors do not measure $I_{DT}$ and $I_{RT}$ as these are difficult and expensive to obtain [13,40] |
| $\alpha$ is represented by the maximum $\alpha$ at solar noon | This maximum $\alpha$ is used in simple PV system design and is considered acceptable since $GSI_T$ is underestimated [13] |
| The sun's orbit is a perfect circle | Allows for the factor of 360/365 to convert the day number ($d$) to a position in the orbit [13] |
| PV system can be fitted on the roof-top | Roof-top PV systems are widely available [13] |
| PV module area ($A_m$) is a function of roof area ($A_r$) | PV modules are to be installed on the roof [13] |
| Humidity, air velocity, dust, shading, ohmic losses of conductors and mismatch losses have no effect on PV performance | Many of these variables are difficult to obtain without experimentation [13,14] |
| $T_c$ is modelled at steady state | This approach was considered more suitable for this study due to lack of data availability |
| *NOCT* model is suitable to determine cell temperature | Gives adequate predicted temperatures for PV applications [17] |
| Grid connection is easily accessible | Grid-connected systems are assessed in this study |
| The extent to which batteries can be charged and discharged is limited by $SOC_{min}$ and $SOC_{max}$ | Depending on the battery technology, full charge or discharge could permanently destroy the battery [29] |
| Battery charge/discharge rates are limited to $I_{Cmax}/I_{Dmax}$ | Battery capacity is affected by the rate at which the battery is charged/discharged [29,31] |
| Monthly *BSD* could be evenly converted to an hourly rate ($BSD_h$) | This is typical practice and allows for hourly assessment [66] |
| 'Cycle life' impact on battery capacity is negligible therefore battery has an absolute lifetime, $N_{batt}$ [29] | Initial assessments of the grid-independent system model for Oman have shown that batteries only go through one complete charge and discharge cycle in a year |
| Charge controller is a standard switched controller | These are the most common controllers used [28] |
| Inverter has an absolute lifetime, $N_{inv}$ | Several studies have assessed inverters as having an absolute lifetime [7,28] |
| $\eta_{inv}$ of grid-connected system is the same as that for grid-independent system | To make both systems comparative to one another |
| $\beta$ can be changed manually on a monthly basis | This is not too time consuming and allows for maximum monthly $P_m$ generation |
| The PV technology is crystalline-silicon | This is a mature technology which dominates the market [13] |
| *NOCT* is set at 48 °C | *NOCT* ranges between 33 °C and 58 °C For a typical module, *NOCT* is 48 °C [18] |
| Battery used is a lead-acid battery | Due to its maturity, familiarity and low cost [43] |
| Battery internal resistance is assumed to be zero and therefore $V_B$ is assumed to remain constant at 48 V | Lead-acid batteries have a very low internal resistance (< 100 milli ohms) [30] For systems greater than 3–4 kWh, it is recommended to set $V_B$ at 48 V [28] |
| Temperature effects on battery voltage and capacity are ignored | Battery is assumed to be stored in-doors at constant temperature |
| $\eta_{voltage}$ is set at 100% therefore $\eta_{Batt}$ is equivalent to $\eta_{coulomb}$ | $V_B$ is constant [29] |
| $SOC_{max}$ is set at 100% and $SOC_{min}$ is set at 30% | Lead-acid batteries can be fully charged while full discharge will permanently destroy the battery [29] |
| $N_{Batt}$ is set at 5 years and $N_{inv}$ is set at 10 years | Typical lifetime of lead-acid batteries and inverters [7,31,74,75] |
| $I_{Cmax}$ and $I_{Dmax}$ are set at C/10 | Charge is added and removed more efficiently at lower currents [29,31] |
| $\eta_{cc}$ is set at 98% | Typical efficiency of charge controller [31] |
| $\eta_{inv}$ is set at 94% | Inverter typically have efficiencies ranging between 92% and 98% [14] |
| $N$ is set at 20 years | Most PV systems have lifetimes ranging between 20 and 25 years [7,13,31,67] |
| Financial exchange rates do not change throughout the system lifetime | Change in exchange rates in the future is difficult to predict |
| Grid power export tariff is the same as the current residential electricity tariff | To date, Oman has no renewable energy policy |
| Behavioural changes in electricity demand as a result of increase in electricity tariff are negligible | Data on behavioural changes in residential electricity demand in Oman are minimal and require extensive data collection and surveys which is beyond the scope of this study |
| Last available data for *GSI* and $T_A$ for the year 2007 are representative of 2013 | The variation of *GSI* and $T_A$ between 2002 and 2013 is small [41,42] |
| $P_D$ for January, February, March and December could be extrapolated | Method devised due to lack of data availability |
| Model villa in Muscat is rectangular | A large portion of the villa archetype in Oman is rectangular [58] |
| Model home wall thickness is 20 cm | This is a standard thickness set by the buildings regulations for Muscat [57] |
| Hourly annual weather and demand data could be repeated annually for 20 years | Due to the lack of hourly data availability, this allows for the modelling of PV systems which typically have a lifetime of 20 years |
| All simulations start on the first day of the month, mid-day | In order to ensure consistency in the results |

## References


[1] AER. Annual report, Tech. rep. Authority of Electricity Generation; 2011/2014.
[2] COWI. Partners, Study on renewable energy resources, Oman. Tech. rep. Authority of Electricity Regulation; 2008.
[3] Parra D, Patel MK. Effect of tariffs on the performance and economic benefits of PV-coupled battery systems. Appl Energy 2016;164:175–87. https://doi.org/10.1016/j.apenergy.2015.11.037.
[4] Dufo-Lopez R, Perez-Cebollada E, Bernal-Agustin JL, Martinez-Ruiz I. Optimisation of energy supply at off-grid healthcare facilities using monte carlo simulation. Energy Convers Manage 2016;113:321–30. https://doi.org/10.1016/j.enconman.2016.01.057.
[5] Shezan SKA, Julai S, Kibria MA, Ullah KR, Saidur R, Chong WT, et al. Performance analysis of an off-grid wind-PV-diesel-battery hybrid energy system feasible for remote areas. J Clean Prod 2016;125:121–32. https://doi.org/10.1016/j.jclepro.2016.03.014.
[6] Yilmaz S, Ozcalik HR, Aksu M, Karapinar C. Dynamic simulation of a PV-diesel-battery hybrid plant for off grid electricity supply. Energy Proc 2015;75:381–7. https://doi.org/10.1016/j.egypro.2015.07.396.
[7] Ghafoor A, Munir A. Design and economic analysis of an off-grid PV system for household electrification. Renew Sustain Energy Rev 2015;42:496–502. https://doi.org/10.1016/j.rser.2014.10.012.
[8] Bastholm C, Fiedler F. Techno-economic study of the impact of blackouts on the viability of connecting an off-grid PV-diesel hybrid system in Tanzania to the national power grid. Energy Convers Manage 2018;171:647–58. https://doi.org/10.1016/j.enconman.2018.05.107.
[9] Khoury J, Mbayed R, Salloum G, Monmasson E. Optimal sizing of a residential PV-battery backup for an intermittent primary energy source under realistic constraints. Energy Build 2015;105:206–16. https://doi.org/10.1016/j.enbuild.2015.07.045.
[10] Ratnam EL, Weller SR, Kellett CM. An optimization-based approach to scheduling residential battery storage with solar PV: assessing customer benefit. Renew Energy 2015;75:123–34. https://doi.org/10.1016/j.renene.2014.09.008.
[11] O. Schmidt, A. Hawkes, A. Gambhir, I. Staffell, The future cost of electrical energy storage based on experience rates, Nature Energydoi:https://doi.org/10.1038/

nenergy.2017.110.
[12] PSE, gPROMs, accessed on 01 January 2014 (2014). URL <http://www.psenterprise.com/>.
[13] Stenning A. Renewing corporate power: a techno-economic assessment of the electricity supply of commercial sector buildings to be renewably resourced in an urban environment case study Thesis London: Imperial Collage; 2014.
[14] Heinrich H. Photovoltaics system design and practice. Wiley; 2012.
[15] Dubey S, Sarvaiya JN, Seshadri B. Temperature dependent photovoltaic (PV) efficiency and its effect on PV poduction in the world; a review. Energy Proc 2013;33:311–21. https://doi.org/10.1016/j.egypro.2013.05.072.
[16] Muzathik AM. Photovoltaic modules operating temperature estimation using simple correlation. Int J Energy Eng 2014;4:151–8.
[17] Trinuruk P, Sorapipatana C, Chenvidhya D. Estimating operating cell temperature of BIPV modules in Thailand. Renew Energy 2009;34:2515–23. https://doi.org/10.1016/j.renene.2009.02.027.
[18] Ross RJ, Smokler M. Flat-plate solar array project final report; 1986. p. 86–31.
[19] Wang Y, Tian W, Ren J, Zhu L, Wang Q. Influence of a building's integrated-photovoltaics on heating and cooling loads. Appl Energy 2006;83:989–1003. https://doi.org/10.1016/j.apenergy.2005.10.002.
[20] Mattei M, Notton G, Cristofari C, Muselli M, Poggi P. Calculation of the polycrystalline PV module temperature using a simple method of energy balance. Renew Energy 2006;31:553–0567. https://doi.org/10.1016/j.renene.2005.03.010.
[21] Jain B, Ansari M, Patil VP. Evaluate PV-panel performance enhancement with matlab. Int J Electr Eng Technol 2014;06:23–37 <http://www.iaeme.com/currentissue.asp?JType=IJEET&VType=6&IType=7> .
[22] Zervas PL, Sarimveis H, Palyvos JA, Markatos NCG. Model-based optimal control of a hybrid power generation system consisting of photovoltaic arrays and fuel cells. J Power Sources 2008;181:327–38. https://doi.org/10.1016/j.jpowsour.2007.11.067.
[23] Jordan DC, Kurtz SR. Photovoltaic degradation rates; an analytical review Tech. rep. National Renewable Energy Laboratory; 2012.
[24] McPherson J. Reliability physics and engineering. Springer; 2013.
[25] Zhu J, Astawa K, Betts T, Gottschalg R. A modelling approach for long-term degradation of thin film silicon photovoltaic modules. Sol Energy Soc. URL <https://dspace.lboro.ac.uk/2134/8167>.
[26] Manuel Vazquez IR-S. Photovoltaic module reliability model based on field degradation studies. Wiley InterScience. doi:https://doi.org/10.1002/pip.825.
[27] Akikur RK, Saidur R, Ping HW, Ullah KR. Comparative study of stand-alone and hybrid solar energy systems suitable for off-grid rural electrification: A review. Renew Sustain Energy Rev 2013;27:738–52. https://doi.org/10.1016/j.rser.2013.06.043.
[28] Kempener R, Lavagne d'Ortigue O, Saygin D, Skeer J, Vinci S, Gielen D. Off-grid PV power systems Tech. rep. IRENA; 2013.
[29] Linden D, Reedy TB. Handbook of batteries. McGraw Hill; 2002.
[30] Jossen A, Garche J, Sauer DU. Operation conditions of batteries in PV applications. Sol Energy 2004;76:759–69. https://doi.org/10.1016/j.solener.2003.12.013.
[31] Jenkins DP, Fletcher J, Kane D. Model for evaluating impact of battery storage on microgeneration systems in dwellings. Energy Convers Manage 2008;49:2413–24. https://doi.org/10.1016/j.enconman.2008.01.011.
[32] Jung J, Tyner WE. Economic and policy analysis for solar PV systems in Indiana. Energy Policy 2014;74:123–33. https://doi.org/10.1016/j.enpol.2014.08.027.
[33] Ma WW, Rasul MG, Liu G, Li M, Tan XH. Climate change impacts on techno-economic performance of roof PV solar system in Australia. Renew Energy 2016;88:430–8. https://doi.org/10.1016/j.renene.2015.11.048.
[34] Rodrigues S, Torabikalaki R, Faria F, Cafofo N, Chen X, Ivaki AR, et al. Economic feasibility analysis of small scale PV systems in different countries. Sol Energy 2016;131:81–95. https://doi.org/10.1016/j.solener.2016.02.019.
[35] Li C, Yu W. Techno-economic comparative analysis of off-grid hybrid photovoltaic/diesel/battery and photovoltaic/battery power systems for a household in Urumqi, China. J Clean Prod 2016;124:258–65. https://doi.org/10.1016/j.jclepro.2016.03.002.
[36] Mac Dowell N, Fajardy M. Inefficient power generation as an optimal route to negative emissions via BECCS? Environ Res Lett. doi:https://doi.org/10.1088/1748-9326/aa67a5.
[37] Goetzberger A, Hoffmann VU. Photovoltaic solar energy generation. Springer; 2004.
[38] Okoye CO, Taylan O, Baker DK. Solar energy potentials in strategically located cities in Nigeria: review, resource assessment and PV system design. Renew Sustain Energy Rev 2016;55:550–66. https://doi.org/10.1016/j.rser.2015.10.154.
[39] Sweetnam T, Al-Maskari B. Re: Oman data, Private communication, type to Al-Saqlawi, J, October 2015.
[40] Al-Zakwani S. Re: Muscat meterological station data, Private communication, Directorate General of Meteorology, type to Al-Saqlawi, J, September 2015.
[41] NCSI. Climate statistics bulletin. Tech. rep., National Centre of Statistics and Information, 2011–2013.
[42] NCSI. Statistical yearbook. Tech. rep. National Centre of Statistics and Information, 2010–2014.
[43] Parra D, Walker GS, Gillott M. Modeling of PV generation, battery and hydrogen storage to investigate the benefits of energy storage for single dwelling. Sustain Cities Soc 2014;10:1–10. https://doi.org/10.1016/j.scs.2013.04.006.
[44] Dynamic, Oman electricity tariffs, accessed on 01 December 2015 (2015). URL <http://www.dynamic-ews.com/Tariffs/Electricity%20Tariffs/Oman.pdf>.
[45] Byrd, How does humidity affect air conditioning and heating, accessed on 06 February 2017 (2013). URL <http://byrdheatingandair.com/articles/how-does-humidity-affect-air-conditioning-and-heating>.
[46] Alex, The Shockley Queisser efficiency limit, accessed on 01 November 2016 (2017). URL http://solarcellcentral.com/limits_page.html.
[47] Cengiz MS, Mamis MS. Price-efficiency relationship for photovoltaic systems on a global basis. Int J Photoenergy. doi:https://doi.org/10.1155/2015/256101.
[48] Nykvist B, Nilsson M. Rapidly falling costs of battery packs for electric vehicles. Nat Clim Change 2014;5:329–32. https://doi.org/10.1038/nclimate2564.
[49] IRENA, The power to change: Solar and wind cost reduction potential to 2025. Tech. rep. International Renewable Energy Agency; 2016.
[50] Krane J. Stability versus sustainability: energy policy in the Gulf monarchies Tech. rep. Cambridge University; 2013.
[51] EIA, Residential electricity prices in Europe and the United States, accessed on 15 May 2016 (2013). URL <http://www.eia.gov/todayinenergy/detail.cfm?id=18851>.
[52] Mayer JN. Current and future cost of photovoltaics Tech. rep. Fraunhofer-Institute for Solar Energy Systems (ISE); 2015.
[53] Pillai U. Drivers of cost reduction in solar photovoltaics. Energy Econ 2015;50:286–93. https://doi.org/10.1016/j.eneco.2015.05.015.
[54] Enerdata, Average electricity consumption per electrified household, accessed on 15 August 2015 (2013). URL <https://www.wec-indicators.enerdata.eu/household-electricity-use.html>.
[55] Al Shehri AM. The Report: Saudi Arabia. Oxford Business Group; 2010.
[56] Segen, Photovoltaic battery guide, accessed on 01 August 2016 (2016). URL <http://www.segen.co.uk/co.uk/batteryguide>.
[57] M. Muncipality, Building regulations for Muscat: Local order no. 23/92; 1992.
[58] Sweetnam T. Residential energy use in Oman: a scoping study. Tech. rep. Passive Systems; 2014.
[59] Anuphappharadorn S, Sukchai S, Sirisamphanwong C, Ketjoy N. Comparison the economic analysis of the battery between lithium-ion and lead-acid in PV stand-alone application. Energy Proc. 2014;56:352–8. https://doi.org/10.1016/j.egypro.2014.07.167.
[60] Mehrabankhomartash M, Rayati M, Sheikhi A, Ranjbar AM. Practical battery size optimization of a PV system by considering individual customer damage function. Renew Sustain Energy Rev 2017;67:36–50. https://doi.org/10.1016/j.rser.2016.08.050.
[61] IEA. Trends 2014 in photovoltaic applications Tech. rep. International Energy Agency; 2014.
[62] IEA. Technology roadmap: solar photovoltaic energy Tech. rep. International Energy Agency; 2014.
[63] Dusonchet L, Telaretti E. Comparative economic analysis of support policies for solar PV in the most representative EU countries. Renew Sustain Energy Rev 2015;42:986–98. https://doi.org/10.1016/j.rser.2014.10.054.
[64] IRENA. Sultanate of Oman, Renewables readiness assessment Tech. rep. International Renewable Energy Agency; 2014.
[65] AER. Existing data report Tech. rep. Authority of Electricity Generation; 2014.
[66] B. University. What does elevated self-discharge do?, accessed on 01 July 2016 (2003). URL <http://batteryuniversity.com/learn/article/elevating_self_discharge>.
[67] Powerthru. Lead acid battery working technical paper, accessed on 11 July 2016 (2016). URL <http://www.power-thru.com/documents/The%20Truth%20About%20Batteries%20-%20Powerthru%20White%20Paper.pdf>.
[68] IRENA. Renewable energy technologies: cost analysis series-solar photovoltaics Tech. rep. International Renewable Energy Agency; 2012.
[69] Dufo-Lopez R, Zubi G, Fracastoro GV. Techno-economic assessment of an off-grid PV-powered community kitchen for developing regions. Appl Energy 2012;91:255–62. https://doi.org/10.1016/j.apenergy.2011.09.027.
[70] Fraunhofer. Photovoltaics report Tech. rep. Fraunhofer Institute for Solar Energy Systems; 2015.
[71] Google, Google shopping-PV panels, accessed on 01 March 2016 (2016). URL <https://www.google.co.uk/>.
[72] Alibaba, Alibaba-PV panels, accessed on 01 March 2016 (2016). URL <www.alibaba.com>.
[73] XE, Currency converter, accessed on 01 April 2016 (2016). URL <http://www.xe.com/currencyconverter/>.
[74] Dufo-Lopez R, Lujano-Rojas JM, Bernal-Agustin JL. Comparison of different lead-acid battery lifetime prediction models for use in simulation of stand-alone photovoltaic systems. Appl Energy 2014;115:242–53. https://doi.org/10.1016/j.apenergy.2013.11.021.
[75] Guinot B, Bultel Y, Montignac F, Riu D, Borgne IN-L. Economic impact of performances degradation on the competitiveness of energy storage technologies-Part 2: application on an example of PV production guarantee. Int J Hydrogen Energy 2013;38:13702–16. https://doi.org/10.1016/j.ijhydene.2013.08.023.